Supersedes RM L50I24
55- 3-29A- (2 copies)

NACA TN 3311
9603

TECH LIBRARY KAFB, NM
0066908

NATIONAL ADVISORY COMMITTEE FOR AERONAUTICS

TECHNICAL NOTE 3311

DESCRIPTION AND ANALYSIS OF A ROCKET-VEHICLE EXPERIMENT ON FLUTTER INVOLVING WING DEFORMATION AND BODY MOTIONS

By H. J. Cunningham and R. R. Lundstrom

Langley Aeronautical Laboratory
Langley Field, Va.

Washington
January 1955

AFMDC
TECHNICAL LIBRARY
AFL 2811

1D

TECH LIBRARY KAFB, NM
0066308

NATIONAL ADVISORY COMMITTEE FOR AERONAUTICS

TECHNICAL NOTE 3311

DESCRIPTION AND ANALYSIS OF A ROCKET-VEHICLE EXPERIMENT ON FLUTTER INVOLVING WING DEFORMATION AND BODY MOTIONS[1]

By H. J. Cunningham and R. R. Lundstrom

SUMMARY

Flight tests and a mathematical analysis were made to demonstrate and confirm a type of subsonic flutter involving rigid-body motions and wing deformations. For the configuration considered, the period of the oscillation was approximately 100 chords per cycle which is well within the range of period found in dynamic-stability work on rigid aircraft with free controls. A mathematical analysis based on two-dimensional incompressible flow provided a conservative prediction of the airspeed at which the low-frequency flutter occurred. It was found that wing bending stiffness is the important parameter for preventing such flutter.

INTRODUCTION

Interaction of deformations of an aircraft structure with the passing airstream can lead to the dynamic instability known as flutter. For bending-torsion wing flutter, the frequency of oscillation is fairly high and usually approaches the natural torsional frequency of the wing in still air. Such an oscillation may be contrasted with ordinary dynamic-stability phenomena involving rigid-body modes which lead to much lower frequencies that are usually controllable.

The fact that the calculated flutter speed may be modified by the addition of free-body modes has been recognized for many years. For example, about 20 years ago it was found analytically (ref. 1) that body mobility had a slight favorable effect on the calculated flutter speed of a particular configuration typical of that day. The problem has from time to time been reconsidered in both American and British literature

---

[1]Supersedes the recently declassified NACA RM L50I29, "Description and Analysis of a Rocket-Vehicle Experiment on Flutter Involving Wing Deformation and Body Motions" by H. J. Cunningham and R. R. Lundstrom, 1950.

and the necessity for determining any potential detrimental effect of special configurations, sweptback wings, higher speeds, and higher altitudes has lately become more insistent. A recent paper by Broadbent (ref. 2) discusses the necessity for including free-body modes in the study of sweptback wings.

Controlled experimentation involving free-body modes is highly desirable although difficult even at low speeds in a wind tunnel. In reference 3 Lambourne gives some experimental results and describes various difficulties encountered, principally the difficulty of supporting the model so that actual flight behavior is sufficiently well simulated. The National Advisory Committee for Aeronautics has been engaged for several years in making flutter experiments in the transonic range by the use of modern telemetering techniques with rocket-powered vehicles. Some of the results of these experiments are given in several NACA papers including references 4 and 5. Such flutter research has been concerned almost entirely with wing bending-torsion flutter. Recently, however, in connection with some of these experiments, flutter failures were obtained which definitely involved much lower frequencies than those obtained in ordinary bending-torsion flutter. A preliminary account of an unexpected low-frequency failure is given in reference 4, and two other low-frequency failures have been observed by W. T. Lauten, Jr., and J. M. Teitelbaum during rocket-propelled model tests at the Langley Pilotless Aircraft Research Station at Wallops Island, Va.

It was decided to repeat the experiment of the D model of reference 4 with more extensive instrumentation in order to obtain information specific to this type of flutter. The present paper includes a description of and results from model D of reference 4 as well as similar and more comprehensive material for the repeat experiment on the model which has been designated model E. Results of an analysis developed on the basis of certain simplifying assumptions are given, and a comparison is made between analytical and experimental results.

SYMBOLS

a nondimensional position of wing elastic axis, $\frac{2x_{ea}}{100} - 1$

$a + x_\alpha$ nondimensional position of wing-section center of gravity, $\frac{2x_{cg}}{100} - 1$

A_g geometric aspect ratio of one exposed wing panel, for rectangular plan-form wings, Length/Chord

b wing semichord, ft

EI bending rigidity, lb-in.^{2}

s nondimensional distance (in wing semichords) from wing midchord line to missile center of gravity measured parallel to missile longitudinal axis, positive when center of gravity is behind wing midchord line

f_{h_1} first-bending natural frequency, cps

f_{h_2} second-bending natural frequency, cps

f_t first-torsion natural frequency, cps

f_α uncoupled first-torsion frequency relative to elastic axis, $f_t\left[1 - \frac{(x_\alpha/r_\alpha)^2}{1 - (f_{h_1}/f_t)^2}\right]^{1/2}$, cps

g_h structural damping coefficient in bending

g_α structural damping coefficient in torsion

g mathematical quantity having qualities of structural damping coefficient

GJ torsional rigidity, lb-in.^{2}

I_{yy} moment of inertia of missile about center of gravity, slug-ft^2

k reduced frequency parameter, $\omega b/v$; π/k is period of oscillation in chords per cycle

l length of wing along leading edge outboard of body, in.

m mass of wing per unit length, slugs/ft

M Mach number

M_{cr} theoretical Mach number at which sonic velocity is first attained over section of wing taken perpendicular to leading edge at zero lift

r_α	nondimensional radius of gyration of wing section about elastic axis $\sqrt{I_\alpha/mb^2}$ where I_α is the mass moment of inertia of wing about its elastic axis per unit length in slug-ft^2/ft
t	time after rocket launching, sec
v	speed, ft/sec
$\frac{v}{b\omega_h}$	nondimensional flutter-speed coefficient
x_{cg}	distance of center of gravity of wing section behind leading edge, percent chord
x_{ea}	distance of wing elastic axis behind leading edge, percent chord
κ	mass ratio, $\pi\rho b^2/m$
κ(stnd.)	value of κ when ρ is standard sea-level density
ρ	air density, slugs/cu ft
ω	angular frequency of vibration, radians/sec
ω_h	angular uncoupled first-bending frequency, radians/sec
ω_α	angular uncoupled first-torsion frequency about elastic axis, $2\pi f_\alpha$, radians/sec
Ω	flutter parameter, $\left(\frac{\omega_h}{\omega}\right)^2(1 + ig)$

EXPERIMENTAL INVESTIGATION

Apparatus and Methods

The test vehicle was essentially a tailless configuration having the test wings as the only stabilizing surfaces in pitch. The model was powered by a modified Aerojet 12AS-1000 D rocket motor capable of carrying it to greater-than-sonic speed with an acceleration of about 4 times gravity. A sketch of model E is shown in figure 1. Center of gravity, weight, and moment of inertia in pitch varied with flight time because of the fuel consumed. These parameters plotted against flight time for model E are shown in figure 2. The launching was made at the Langley Pilotless Aircraft

Research Station at Wallops Island, Va., from a near-zero-length launcher, as described in reference 5. Photographs of model E in the launching position are shown in figure 3. The test wings were made of laminated white pine with an inlay of 0.032-inch 24S-T aluminum alloy to duplicate as closely as possible the test wings of model D of reference 4. Strain gages were mounted on the elastic axes of the wings 4 inches from the wing root, as shown in figure 1.

A six-channel telemeter was installed in the model with instrumentation to give continuous readings of the strains, left-wing bending, right-wing bending, and right-wing torsion, at the corresponding gage locations and also to give continuous readings of longitudinal and normal accelerations of the model center of gravity and angle of attack of the missile. Speed of the model was obtained by integration of longitudinal acceleration, and the altitude was obtained from a pulse-type tracking radar unit. Atmospheric conditions prevailing at the time of flight were obtained from a radiosonde.

The accuracy of the quantities measured is believed to be within the following limits: longitudinal and normal accelerations, 2 percent; velocity, 4 percent; wing bending and twisting moments, 20 percent; and phase angle between any two quantities, 15°.

Experimental Results

The physical characteristics of the wings as determined by preflight ground tests are listed in table I. Data for model E are presented in figures 4 to 7 as functions of the flight time. Included in these figures are the available data for model D from reference 4 for comparison. Figure 4 includes flight velocities; figure 5 shows Mach number and air density; figure 6 shows longitudinal acceleration. Figure 7 presents the following data: bending moments of both wings (positive, wing bent down) at the strain-gage locations, twisting moment of the right wing about its elastic axis (positive, leading edge up) at the strain-gage location, and normal acceleration of the missile center of gravity (positive, up). It was desired to obtain the angle of attack of model E directly as a function of time, but the angle-of-attack indicator was inoperative during flight. As a result, the angle of attack was determined by use of the normal acceleration and an assumed lift-curve slope of 0.08 per degree as obtained from lifting-surface theory.

Comparison of figure 7 for model E and figure 9 of reference 4 for model D indicates that both flights had similar behavior. At a speed of about 400 feet per second, there began pitching oscillations with slowly increasing amplitudes which continued to a speed of about 620 feet per second for model D and 500 feet per second for model E. Over this interval the primary frequencies of oscillation increased from 4 to 7 cycles per

second for model E and from 5 to 8 cycles per second for model D, and there was a considerable component of the wing first-bending natural frequencies present on the wing bending strain-gage traces. An interruption or damping of the oscillations then occurred and was followed by final divergent oscillations with frequencies of about 9.0 cycles per second for model D and 8.5 cycles per second for model E which resulted in failures of the wing after about 7 or 8 cycles. The final oscillations were of a much more regular character and approached a divergent sine wave. The speeds at the beginning of the final divergent oscillations, 670 feet per second for model D and 580 feet per second for model E, are considered to be the experimental flutter speeds because of the regularity of the subsequent oscillations. As indicated by the time histories, the periods of the low-frequency oscillations for both models, from the beginning of a detectable oscillation until wing failure, were about 100 chords per cycle.

The primary interest in flutter research centers on the speed and frequency of oscillation. A secondary interest exists in the deflection amplitudes and in the phase relationships of the various motions; the latter are usually not experimentally determinable with good accuracy. From analysis of the oscillograph records of model E taken during flutter over the interval $t = 5.40$ seconds to 5.65 seconds, the amplitudes of wing deformation and body motions relative to a wing-tip-bending amplitude of 1 inch were found to average about 0.0065 radian for wing-tip torsion, 0.020 radian for pitching, and 0.21 inch for vertical translation. The wing-tip-bending and wing-tip-torsion amplitudes were determined through the assumption of a constant lift distribution from wing tip to wing tip, whereas the amplitude of vertical translation was obtained by integrating the normal acceleration twice. The body-pitching amplitudes were determined by using the normal acceleration and an assumed lift-curve slope of 0.08 per degree. The overall accuracy of the experimentally determined amplitudes is thought to be within ±50 percent; thus, these values are at least of the proper order of magnitude.

It can be seen from figure 7 that the phase relationship is as follows within the limit $\pm 15^{\circ}$ of experimental accuracy: At an instant when the wing is bent up a maximum amount, it is also twisted (leading edge up) a maximum amount and, as interpreted from the normal acceleration, the missile is pitched nose up and translated down a maximum amount.

ANALYTICAL INVESTIGATION

Bases of Analysis

Only an outline of the analytical treatment used to obtain the results is given here. It is assumed that the theory of linear superposition for small disturbances holds. A simplified configuration which has four degrees

of freedom in a symmetric oscillation is treated. There are two rigid-body degrees of freedom: pitching about the center of gravity, and vertical translation; and two wing-deformation degrees of freedom which are approximated by the first-uncoupled-bending and first-uncoupled-torsion modal shapes of an ideal uniform cantilever beam. For convenience, the aerodynamic coefficients used for a wing section are those of incompressible, two-dimensional potential flow and yield forces which are proportional to the displacement and motion of that section (strip analysis). Spanwise distributions of air forces due to symmetric motions of a rigid body are thus constant in magnitude and phasing from wing tip to wing tip, including the body intercept. In view of the Mach number of the experimental flutter, which is well below the critical Mach number M_{cr} of the airfoil section, aerodynamic coefficients for incompressible flow are considered satisfactory. Coefficients for compressible flow could be substituted, however.

The configuration has no other horizontal airfoil surface and no other aerodynamic forces are assumed on the body. Each half-wing is uniform and the two half-wings, right and left, of each missile are treated as being identical. The effect of gravity on an oscillation having the frequency of the observed oscillation is considered negligible, as are the effects of rocket thrust.

Equations of Equilibrium

In order to obtain the theoretical conditions for flutter, Lagrange's equation is employed, as, for example, in reference 6, to derive four equations of equilibrium. With the use of the specified condition of harmonic motion, the four equations may be written in matrix form as follows:

$$\begin{bmatrix} a_{11} & a_{12} & a_{13} & a_{14} \\ a_{21} & a_{22} & a_{23} & a_{24} \\ a_{31} & a_{32} & a_{33} & a_{34} \\ a_{41} & a_{42} & a_{43} & a_{44} \end{bmatrix} \begin{bmatrix} x_1 \\ x_2 \\ x_3 \\ x_4 \end{bmatrix} = \begin{bmatrix} \Omega x_1 \\ \Omega \left(\frac{\omega_\alpha}{\omega_h}\right)^2 x_2 \\ \Omega p x_3 \\ \Omega T x_4 \end{bmatrix} \tag{1}$$

In this equation the quantity $\Omega = \left(\frac{\omega_h}{\omega}\right)^2 (1 + ig)$ where g has the properties of a structural damping coefficient. (Structural damping force

is proportional to amplitude and in phase with velocity.) The quantities x_1, x_2, x_3, and x_4 represent the nondimensional amplitudes of oscillation in wing bending, wing torsion, body pitching, and vertical translation, respectively. On the basis of the foregoing assumptions, for the configuration treated,

$$a_{11} = \frac{1}{\kappa} - A_{ch}$$

$$a_{12} = 1.3558\left(\frac{x_\alpha}{\kappa} - A_{c\alpha}\right)$$

$$a_{13} = 1.5662\left(\frac{-s + a + x_\alpha}{\kappa} - A_{cp}\right)$$

$$a_{14} = 1.5662a_{11}$$

$$a_{21} = 0.6778\left(\frac{x_\alpha}{\kappa} - A_{ah}\right)$$

$$a_{22} = \frac{r_\alpha^2}{\kappa} - A_{a\alpha}$$

$$a_{23} = 1.2732\left[\frac{r_\alpha^2}{\kappa} + \frac{(-s + a)x_\alpha}{\kappa} - A_{ap}\right]$$

$$a_{24} = 1.8784a_{21}$$

$$a_{31} = 0.33177\left(\frac{-s + a + x_\alpha}{\kappa} - A_{dh}\right)$$

$$a_{32} = 0.5395\left[\frac{r_\alpha^2}{\kappa} + \frac{(-s + a)x_\alpha}{\kappa} - A_{d\alpha}\right]$$

$$a_{33} = \frac{r_p^2}{\kappa} - A_{dp}$$

$$a_{34} = -A_{dh}$$

$$a_{41} = 0.33177a_{11}$$

$$a_{42} = 0.39793a_{12}$$

$$a_{43} = -A_{cp}$$

$$a_{44} = \frac{1}{\kappa_T} - A_{ch}$$

where

$$A_{ch} = A_{ch}(k) = -1 - \frac{2G}{k} + i\frac{2F}{k}$$

$$A_{c\alpha} = A_{c\alpha}(k,a) = a + \frac{2F}{k^2} - \left(\frac{1}{2} - a\right)\frac{2G}{k} + i\left[\frac{1}{k} + \frac{2G}{k^2} + \left(\frac{1}{2} - a\right)\frac{2F}{k}\right]$$

$$A_{ah} = A_{ah}(k,a) = -\frac{1}{2} - \left(\frac{1}{2} + a\right)A_{ch}$$

$$A_{a\alpha} = A_{a\alpha}(k,a) = -\frac{1}{8} - a^2 - \left(\frac{1}{2} + a\right)\frac{2F}{k^2} + \left(\frac{1}{4} - a^2\right)\frac{2G}{k} + i\left[\left(\frac{1}{2} - a\right)\frac{1}{k} - \left(\frac{1}{4} - a^2\right)\frac{2F}{k} - \left(\frac{1}{2} + a\right)\frac{2G}{k^2}\right]$$

$$A_{cp} = A_{c\alpha}(k,s)$$

$$A_{dh} = A_{ah}(k,s)$$

$$A_{dp} = A_{a\alpha}(k,s)$$

$$A_{ap}(k,a,s) = A_{a\alpha} - (s - a)A_{ah}$$

$$A_{d\alpha}(k,a,s) = A_{a\alpha} - (s - a)A_{c\alpha}$$

and

$$\frac{r_p^2}{\kappa} = \frac{\text{Mass moment of missile in pitch about its center of gravity}}{(\text{Span})\pi\rho b^4}$$

$$\frac{1}{\kappa_T} = \frac{\text{Total mass of missile}}{(\text{Span})\pi\rho b^2}$$

The quantity a is the nondimensional distance (in wing semichords) from the wing midchord line to the wing elastic axis, positive when the elastic axis is behind the midchord. The quantity s is the nondimensional distance (in wing semichords) from the wing midchord line to the center of gravity of the missile, positive when the center of gravity is behind the midchord. The quantities F and G are the real and imaginary parts, respectively, of the complex function $C = C(k) = F(k) + iG(k)$ developed in reference 7. The reduced frequency parameter k equals $\frac{\omega b}{v}$.

It is to be recognized that equation (1) represents a characteristic-value problem of aeroelastic harmonic motion. The a_{ij}'s depend on the reduced frequency k, whereas Ω contains the frequency ω. Combinations of ω and k which result in a specified value of g are the characteristic values (eigenvalues) of the system. Knowledge of k and ω leads to a flutter speed v. The trivial solution $x_1 = x_2 = x_3 = x_4 = 0$ is, of course, not sought.

The quantities p and T are proportional to any mechanical restoring force due to body motions in the body-pitching and vertical-translation degrees of freedom, respectively. Such restoring forces could exist, for example, if the model were mounted on springs in a wind tunnel. When the wing-body combination is of the freely flying type, however, there is no mechanical restoring force; that is, the natural (in vacuo) frequencies of the two rigid-body degrees of freedom are zero. Hence, the characteristic-value solutions for equation (1) are sought at the limit as p and T approach zero.

DISCUSSION AND COMPARISON OF ANALYTICAL AND EXPERIMENTAL RESULTS

Rayleigh-Ritz Treatment in Four Degrees of Freedom

When equation (1) for harmonic motion is treated in the Rayleigh-Ritz manner there exist in general four roots of flutter speed and frequency which satisfy the equations of equilibrium, although one or more roots may have no physical significance. For the configuration tested and analyzed, the critical (lowest) flutter speed root (designated root A) corresponds to an oscillation involving appreciable proportions of the rigid-body stability modes at a frequency which is a fraction of the wing first-bending natural frequency. The next higher speed root (designated root B) corresponds to the conventional wing flexure-torsion flutter and only minute amplitudes of rigid-body motions are present.

During the flight time after launching, several flutter parameters were continually changing. Such varying parameters were: air density, weight and mass moment in pitch of the missile, and the location of the missile center of gravity. These combined changes have only a moderate effect, an increase of about 7 or 8 percent, on the calculated flutter speed (root A) from $t = 0$ to the time of wing failure. The calculated flutter speeds as functions of time are included in figure 4. (The corresponding changes in flutter frequencies, amplitude ratios, and phasings are also small.) The intersections of calculated flutter speeds and flight speeds give the predicted flutter speeds, 520 feet per second for model D and 435 feet per second for model E, as shown in figure 4. The corresponding predicted flutter frequencies are 6.0 cycles per second for model D and 4.3 cycles per second for model E. Each configuration did not flutter, however, until its flight speed was 30 percent higher, 670 feet per second for model D and 580 feet per second for model E, as also shown in figure 4. Thus, the analysis was conservative in its predictions of flutter speeds.

With regard to the degree of conservatism of the analytically predicted flutter speeds it should be pointed out that, even though the aspect ratio is 7 (including body intercept), the finite-span correction

to the flutter speed is large for small values of the reduced frequency parameter k. For models D and E, the analytical value of k was approximately 0.027 which is small for flutter work. Reference 8 gives some results of flutter tests made in part to determine the effect of finite aspect ratio on the flutter of cantilever wings. The flutter was the bending-torsion type and occurred mostly in a range of k from about 0.15 to 0.30. According to the results of reference 8 for an aspect ratio of 6 to 8, the finite span causes an increase of roughly 5 to 10 percent in the flutter speed. For such a low value of k as was obtained with models D and E, it is known that the finite span causes a considerably larger increase in the flutter speed. Therefore, it appears that, if the proper finite-span corrections were made, an analytically predicted flutter speed would agree much better with the experimentally determined one. Compressibility effects also influence the results and can be taken into account. It is of interest to note that an oscillation with $k = 0.027$ has a period of 117 chords per cycle since π/k equals the period. This value of the period is well within the range of period treated in dynamic-stability work with rigid or undeformable aircraft.

The amplitude ratios and phasing of the various degrees of freedom associated with root A for model E when $t = 5.2$ seconds based on a wing-tip-bending amplitude of 1 inch are as follows:

Degree of freedom	Relative amplitude	Relative phase angle, deg
Wing-tip bending	1.0000 inch	0
Wing-tip torsion	.00436 radian	179.1
Rigid-body pitching	.01679 radian	186.1
Rigid-body vertical translation	.2437 inch	186.0

The parameters used were: mass moment of missile in pitch, 13.25 slug-feet^2; weight of missile, 211 pounds; air density, 0.002260 slug per cubic foot; and the parameters of the right wing of model E. The wing-tip-torsion amplitude is one-quarter of the body-pitching amplitude, and the vertical translation amplitude is one-quarter of the wing-tip-bending amplitude. Each degree of freedom is very nearly in phase or almost diametrically out of phase with other degrees of freedom, (on the basis that positive translation and wing bending are downward, whereas positive angular displacement is leading edge or nose up). Also of interest is the virtual identity of phasing of the two rigid-body modes, which fact, together

with the appropriate amplitude ratios, indicates that the missile is pitching effectively about a lateral axis 14.9 inches forward of the missile center of gravity. All the analytical amplitude ratios and phase relationships agree with their experimental counterparts (reported in section entitled "Experimental Results") within the experimental accuracy.

The amplitude ratios of wing flexure-torsion flutter (root B), based on a wing-tip-bending amplitude of 1 inch, are minute for the two body degrees of freedom, whereas the wing-tip-torsion amplitude is 0.0676 radian with a phasing of about -18°. The ratio of body weight to wing weight ranged from 38 at time of launching to 31 at time of wing failure for model E; if this ratio were smaller, more relative body motion might be associated with root B.

Effect of Various Binary and Ternary Combinations of Freedoms

Analyses employing various binary and ternary combinations of degrees of freedom were made and the results were compared with those of the four-degree-of-freedom analysis. Results are given in table II. The parameters used throughout are those of the right wing of model D and those listed at the top of table II. The four-degree-of-freedom analysis is designated type (a).

Consider root A. The addition of the wing-torsion degree of freedom to an analysis not already including it corresponds to a reduction of torsional stiffness from an infinite value to the finite experimentally determined value. Even though the amplitude of wing-tip torsion in a four-degree-of-freedom analysis, type (a), is small compared with body-pitching amplitude, addition of wing torsion to analysis types (c) or (e) so that they become type (d) or (a), respectively, causes a significant reduction of about 13 percent in the analytically determined flutter speed. These reductions indicate that it is potentially dangerous to exclude the wing torsion from an analysis of body-freedom flutter. The addition of the vertical-translation degree of freedom to analysis type (c) or (d), so that analysis type (e) or (a), respectively, is obtained, effects an increase of 50 percent in the flutter speed and demonstrates clearly that it is not realistic to exclude vertical translation from an analysis treating body freedoms, at least for the present configuration. Thus, it seems clear that at least the four degrees of freedom employed in this report should be included in an analysis of symmetrical body-freedom flutter. The wing-bending stiffness is of predominant importance to the flutter speed for root A inasmuch as that flutter speed is virtually directly proportional to the natural bending frequency, at least in the range of low ratio of bending frequency to torsion frequency.

The flutter speed and frequency of root B, primarily wing bending-torsion flutter, are unchanged regardless of which type of analysis, (a),

(b), or (d), is employed, and for root B the flutter speed is predominantly affected by the torsional stiffness in contrast with the predominant effect of bending stiffness on the flutter speed of root A.

Effect of Relative Positions of Wing and Missile Center of Gravity

Another variable whose effect was studied was the distance from the missile center of gravity to the wing leading edge. The flutter parameters used were again those of the right wing of model D and those listed in table II except for the fixed distance between the wing leading edge and missile center of gravity. The analysis was type (a); that is, it included all four degrees of freedom.

Figure 8 shows the two calculated roots A and B of flutter-speed coefficient as a function of the distance of the wing leading edge behind the center of gravity of the missile. The experimental flutter-speed coefficient for model D is included in the figure at a wing position of 3.38 semichords, even though the experimental parameters differed slightly or moderately from those at the top of table II on which the analytical curves are based. If the parameters of the analysis coincided with their experimental counterparts, the calculated curves would be affected by only a few percent. The important point is that the experimental flutter speed is about 30 percent higher than the calculated one. It is pertinent to recall that the missile has no horizontal airfoil surface other than the wing and that the missile would become statically unstable with the wing very far forward near the center of gravity. Such a rigid-body static instability is not indicated in the figure. Two low-frequency failures of missiles which did have horizontal tails and which had the missile center of gravity at approximately one-eighth chord have been observed during rocket-propelled model tests made at the Langley Pilotless Aircraft Research Station at Wallops Island, Va.

If analysis types (c) or (d) (see table II) which do not include the freedom of vertical translation were employed, it would be predicted, on the basis of the aerodynamic forces of two-dimensional incompressible potential flow developed in reference 7, that single-degree-of-freedom rigid-body pitching instability would be encountered over the approximate range of wing position shown in figure 8. This single-degree pitching instability was investigated analytically by Smilg in reference 9. The quantity $I_\alpha/\pi\rho b^4$ of reference 9 (where I_α represents the mass moment in pitch of the missile divided by the span) is about ten to eleven thousand for models D and E. The predicted borderline flutter speed (root A), if no vertical translation were permitted, would be zero in the critical range of wing location, since no mechanical restraint of pitching exists; that is, the in-vacuo natural rigid-body pitching frequency is

zero. It appears, however, that such an unhappy possibility is precluded, even in two-dimensional incompressible flow, by the actual existing freedom of vertical translation of the missile in flight, at least for the configuration treated.

The two low-frequency failures of missiles observed during the rocket-propelled model tests mentioned previously will now be considered. Each of these models had a pair of unswept rectangular uniform model wings 24 inches by 8 inches. For convenience, the models are designated models 6 and 7. The wings of model 6 were designed to be similar to, although slightly smaller than, the wings of models D and E of the present report, and the wing first-bending and first-torsion frequencies of model 6 were practically identical to those of model D. The leading edges of the wings of models 6 and 7 were located slightly ahead of the missile center of gravity, -0.25 semichord for model 6 and -0.38 semichord for model 7. The complete models 6 and 7 had weights and mass moments in pitch approximately one-third as great as those of models D and E. Each model included a horizontal tail having an area equal to about 20 percent of the wing area, and a tail length of about one-quarter of the total tip-to-tip wing span.

Thus, it may be seen that models 6 and 7, except for the added horizontal tails, were dynamically fairly similar to a hypothetical model D or E which has had its wings moved forward near to the missile center of gravity. In the light of such observation, it is interesting to examine figure 8 for a small negative value of the abscissa or wing position. In that region the speed of the flutter involving body motions is predicted to be lower than the speed for wing bending-torsion flutter of a modified model D or E.

All these circumstances lead to the conjecture that the horizontal-tail volumes of models 6 and 7 were sufficiently large to prevent a static instability, but not sufficient, or the tails were improperly placed, to prevent a low-frequency body-freedom flutter.

CONCLUSIONS

The following conclusions may be drawn from flight tests and a mathematical analysis made to investigate a type of flutter involving wing deformation and body motions of a particular configuration and certain modifications of that configuration:

1. The possibility of a flutter type of dynamic instability involving appreciable proportions of rigid-body motions as well as wing structural deformations has been predicted analytically and confirmed experimentally. The flutter was entirely different from conventional wing bending-torsion flutter in that the frequency was about one-half

the wing first-bending natural frequency. The period was approximately 100 chords per cycle which is well within the range of period found in rigid-body control-free stability work.

2. A flutter analysis based on two-dimensional incompressible flow provided a conservative (by 30 percent) prediction of the airspeed at which the flutter would occur for the configuration studied.

3. Wing-bending stiffness rather than wing-torsional stiffness has the predominant effect on speed of the body-freedom flutter.

4. At least four degrees of freedom, wing bending, wing torsion, body pitching, and body vertical translation, should be included in an analysis of symmetrical flutter involving wing deformations and body motions.

5. The analysis predicted that, if the wing were moved rearward from a position of coincidence of wing quarter chord and missile center of gravity (no horizontal tail present), the speed of flutter involving body motions would first decrease sharply until a certain wing position relative to the center-of-gravity location was reached and then would increase slowly as the wing was moved farther to the rear.

Langley Aeronautical Laboratory,
National Advisory Committee for Aeronautics,
Langley Field, Va., September 28, 1950.

REFERENCES

1. Frazer, R. A., and Duncan, W. J.: Wing Flutter As Influenced by the Mobility of the Fuselage. R. & M. No. 1207, British A.R.C., 1929.

2. Broadbent, E. G.: Some Considerations of the Flutter Problems of High-Speed Aircraft. Sec. International Aero. Conference, N. Y., 1949, pp. 556-581.

3. Lambourne, N. C.: An Experimental Investigation on the Flutter Characteristics of a Model Flying Wing. R. & M. No. 2626, British A.R.C., 1952.

4. Lundstrom, Reginald R., Lauten, William T., Jr., and Angle, Ellwyn E.: Transonic-Flutter Investigation of Wings Attached to Two Low-Acceleration Rocket-Propelled Vehicles. NACA RM L8I30, 1948.

5. Angle, Ellwyn E.: Initial Flight Test of the NACA FR-1-A, a Low-Acceleration Rocket-Propelled Vehicle for Transonic Flutter Research. NACA RM L7J08, 1948.

6. Barmby, J. G., Cunningham, H. J., and Garrick, I. E.: Study of Effects of Sweep on the Flutter of Cantilever Wings. NACA Rep. 1014, 1951. (Supersedes NACA TN 2121.)

7. Theodorsen, Theodore: General Theory of Aerodynamic Instability and the Mechanism of Flutter. NACA Rep. 496, 1935.

8. Widmayer, E., Jr., Lauten, W. T., Jr., and Clevenson, S. A.: Experimental Investigation of the Effect of Aspect Ratio and Mach Number on the Flutter of Cantilever Wings. NACA RM L50C15a, 1950.

9. Smilg, Benjamin: The Stability of Pitching Oscillations of an Airfoil in Subsonic Incompressible Potential Flow. MR No. MCREXA5-4595-8-3, Air Materiel Command, Eng. Div., U. S. Air Force, Mar. 19, 1948.

TABLE I

WING PARAMETERS

Parameters	Model D		Model E	
	Left wing	Right wing	Left wing	Right wing
Airfoil section	NACA 65A006	NACA 65A006	NACA 65A006	NACA 65A006
M_{cr}	0.84	0.84	0.84	0.84
l, in.	29.875	29.875	30	30
A_g	3	3	3	3
b, ft	0.419	0.419	0.417	0.417
x_{cg}, percent chord	38.8	37.6	40.0	40.94
x_{ea}, percent chord	33.5	35.2	36.75	37.5
a	-0.33	-0.296	-0.265	-0.25
$a + x_\alpha$	-0.224	-0.248	-0.20	-0.1812
$\frac{l}{\kappa\ (\text{stnd.})}$	24.6	25.1	31.11	31.08
r_α^2	0.2255	0.2105	0.183	0.1837
f_{h_1}, cps	19.5	20	16	16.5
f_{h_2}, cps	115.0	115.5	99	106
f_t, cps	134	138.5	118.5	119
f_α, cps	131	137.5	117.0	117.5
GJ, lb-in.^{2}	3.36×10^5	3.61×10^5	2.552×10^5	2.555×10^5
EI, lb-in.^{2}	2.76×10^5	2.93×10^5	2.31×10^5	2.34×10^5
g_h	0.05	----------	0.04	0.04
g_α	0.01	0.02	----------	0.01

TABLE II

MISSILE PARAMETERS

[Missile center of gravity is 17 inches ahead of wing leading edge; missile mass moment in pitch is 14.8 slug-ft^2; missile weight is 236 lb; air density ρ is 0.002272 slug per cu ft.]

Type of analysis	Degrees of freedom included (1)				Flutter-speed coefficient, $v/b\omega_h$		Flutter frequency ratio, ω/ω_h	
					Root A (2)	Root B (3)	Root A	Root B
a	F	T	P	V	9.6	22.5	0.26	3.40
b	F	T	-	-	----	22.5	----	3.40
c	F	-	P	-	7.3	----	0.20	----
d	F	T	P	-	6.4	22.5	0.17	3.40
e	F	-	P	V	11.2	----	0.287	----

[1]Designation of degrees of freedom
F - wing flexure (first bending)
T - wing torsion (first torsion)
P - rigid-body pitching
V - rigid-body vertical translation

[2]Root A - critical body-freedom root

[3]Root B - critical wing bending-torsion root

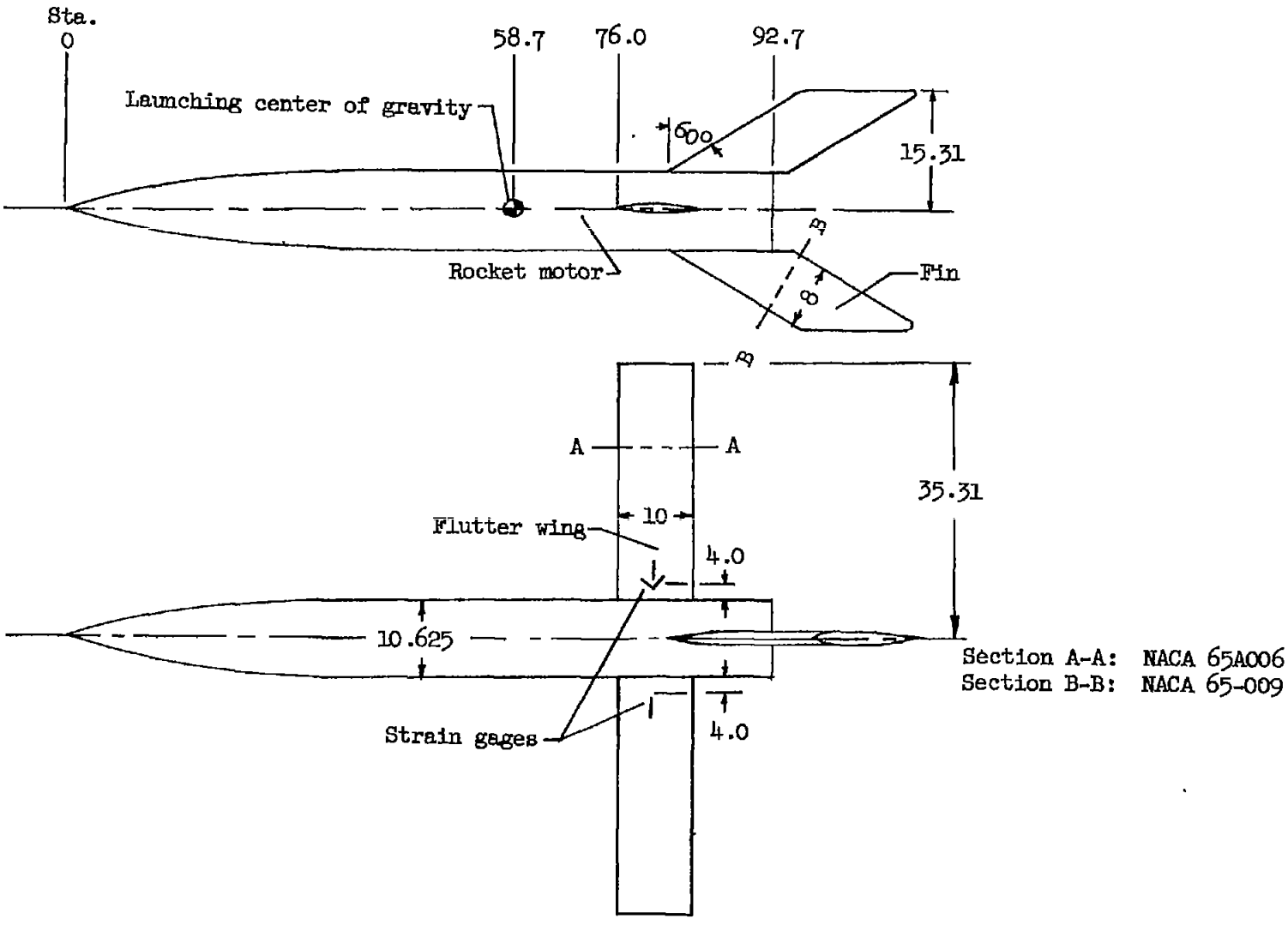

Figure 1.- Layout of flutter test vehicle, model E. All dimensions are in inches.

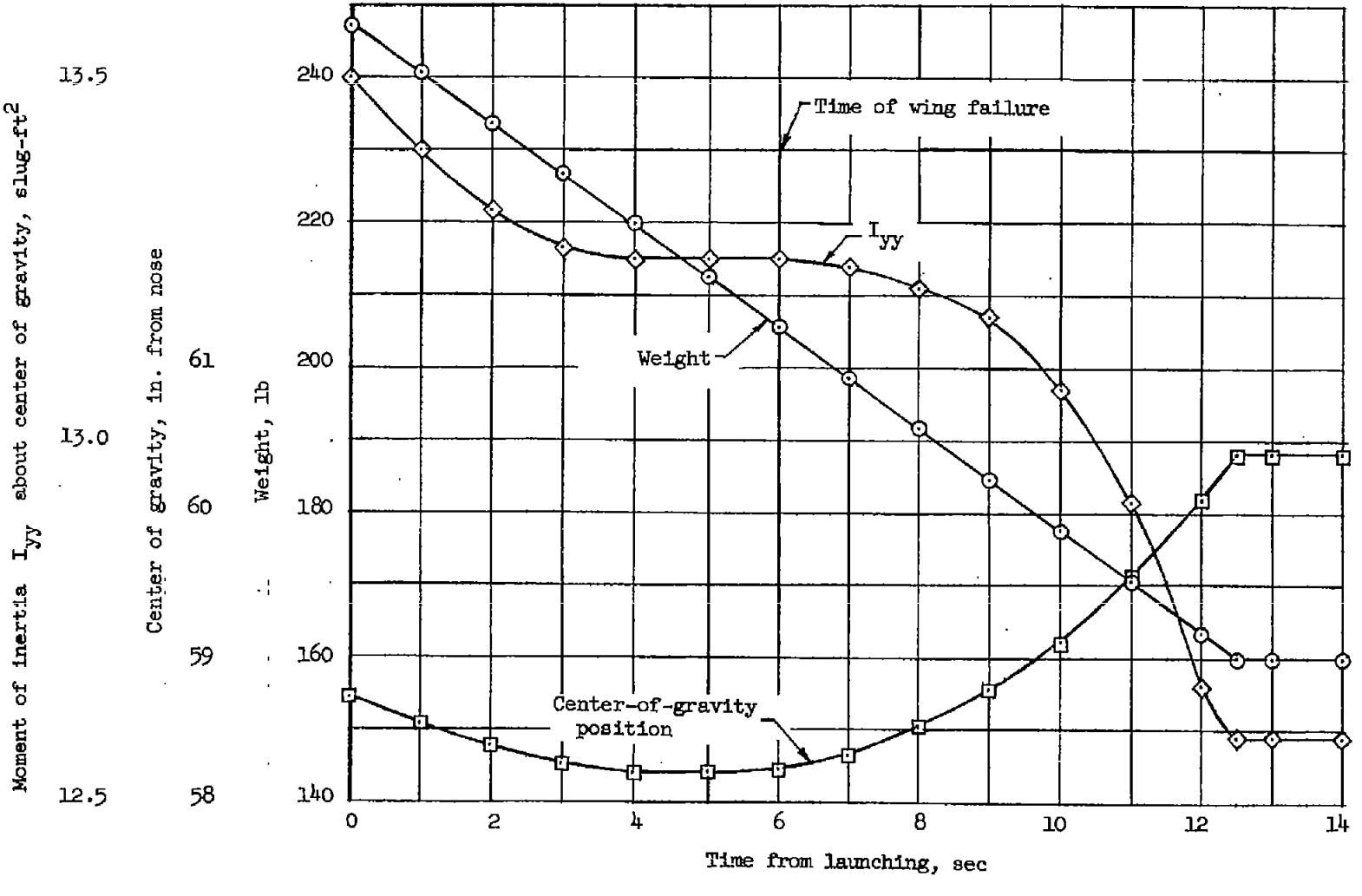

Figure 2.- Variations of model E parameters with time.

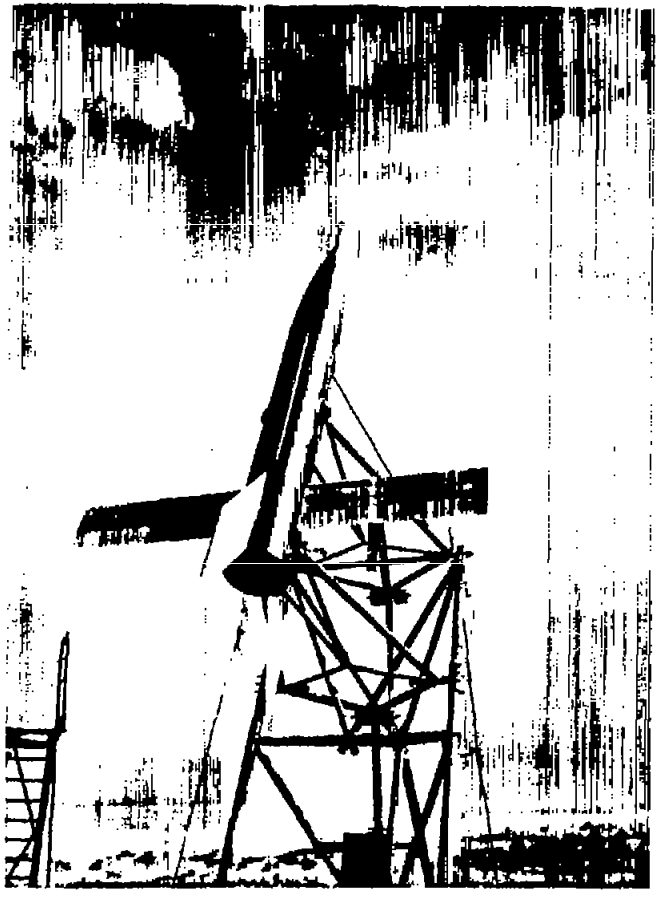

L-60482

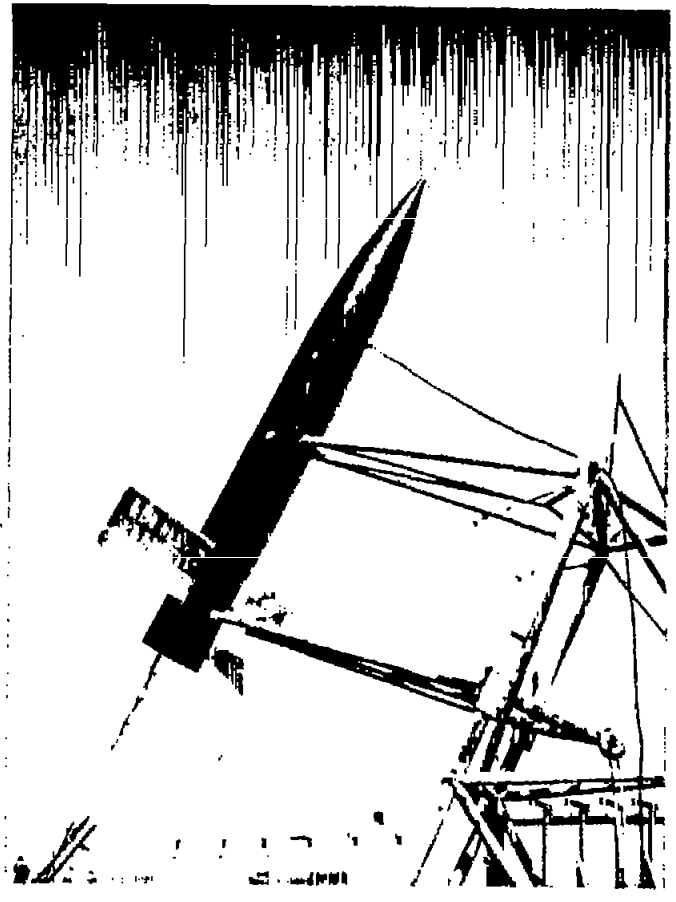

L-60483

Figure 3.- Model E in launching position.

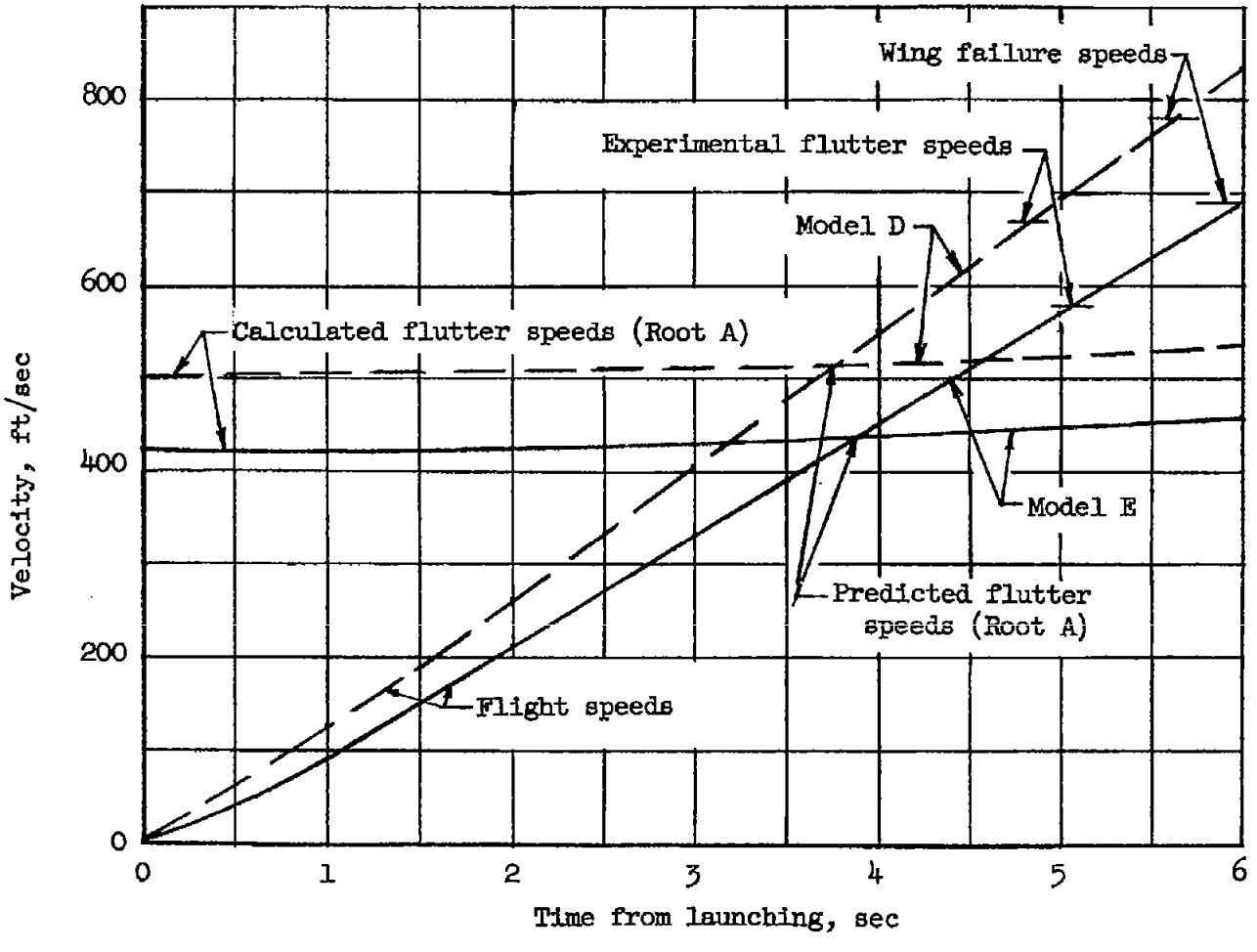

Figure 4.- Velocity plotted against time.

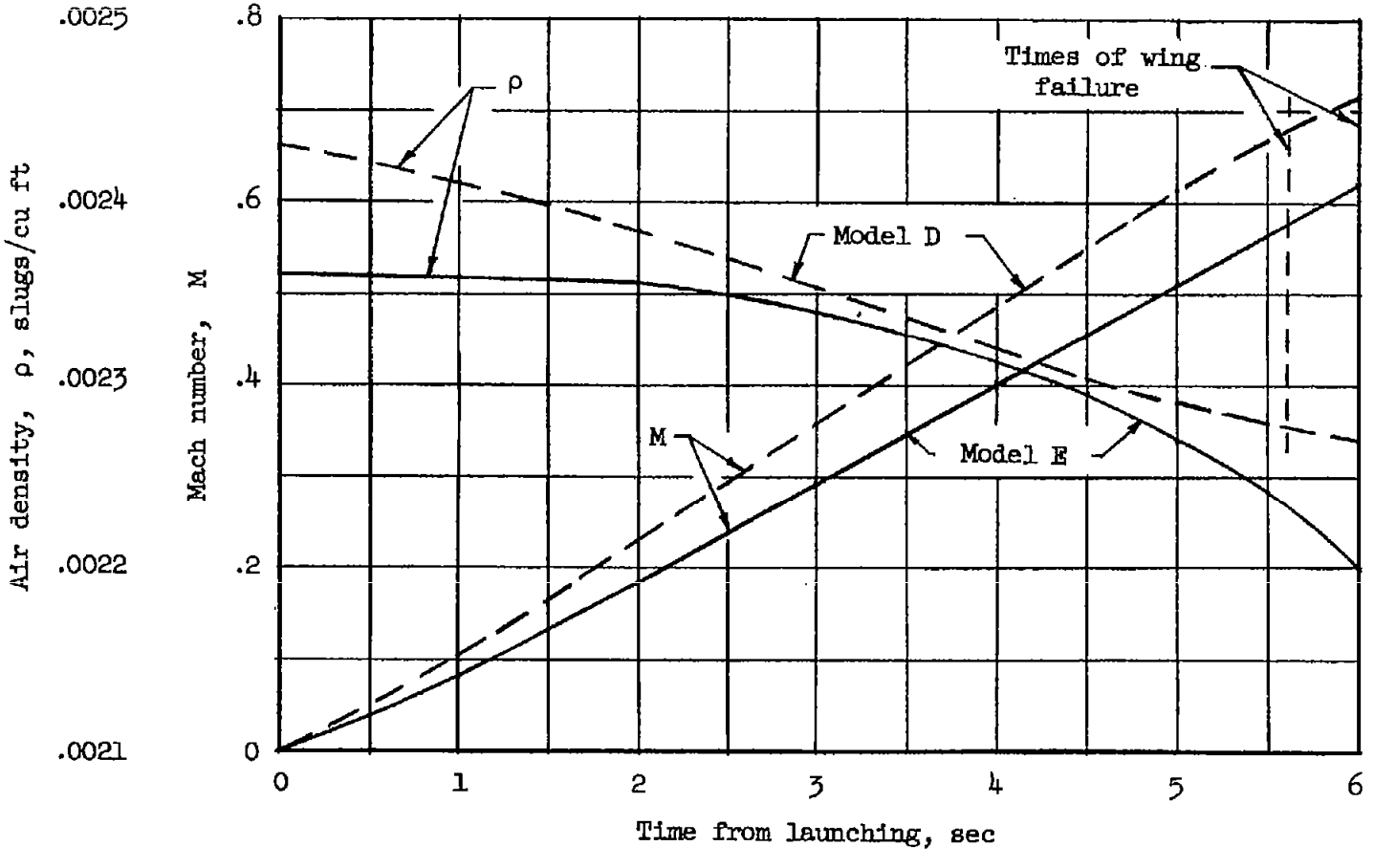

Figure 5.- Air density and Mach number variations with time.

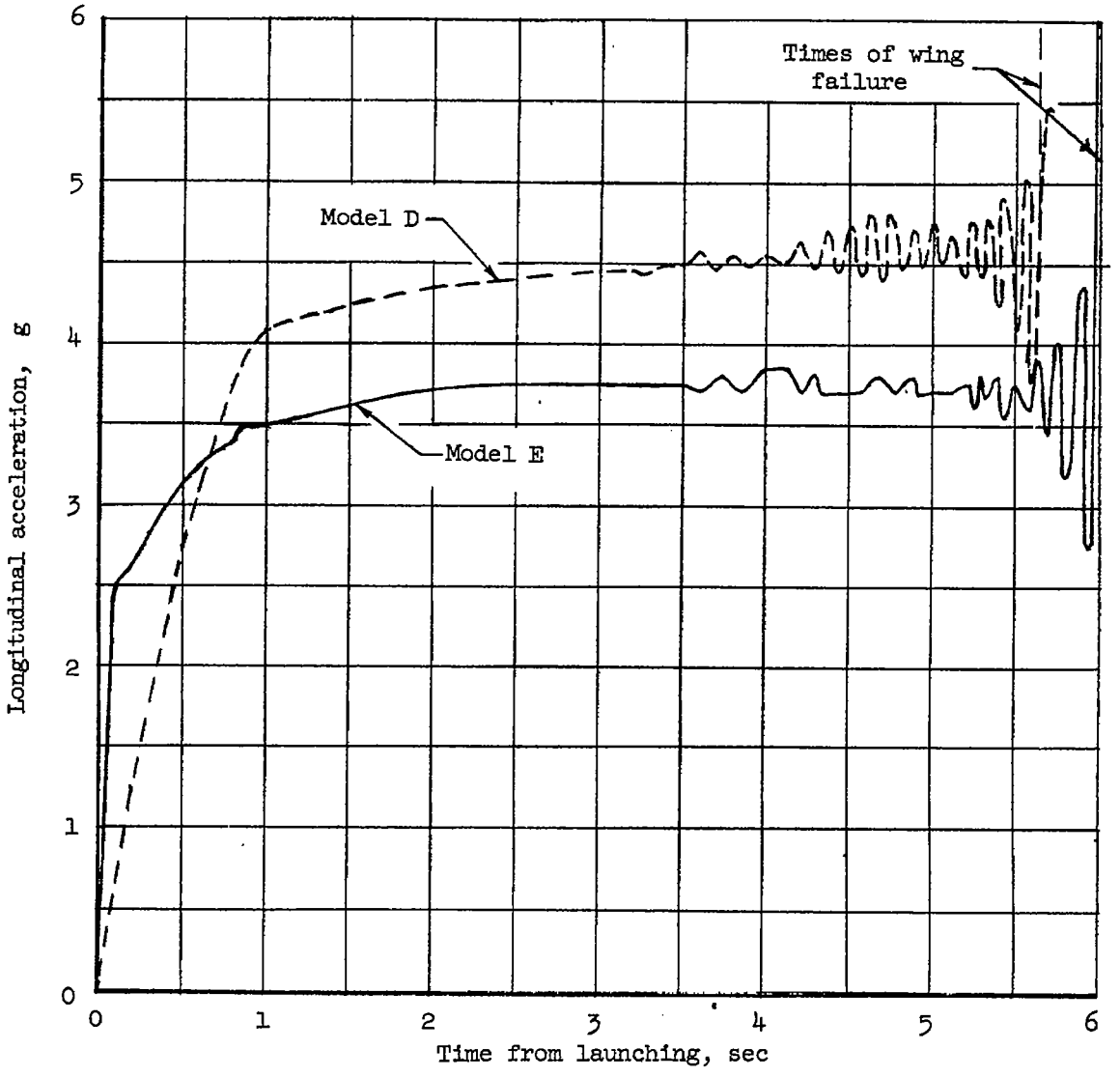

Figure 6.- Variations of longitudinal acceleration with time.

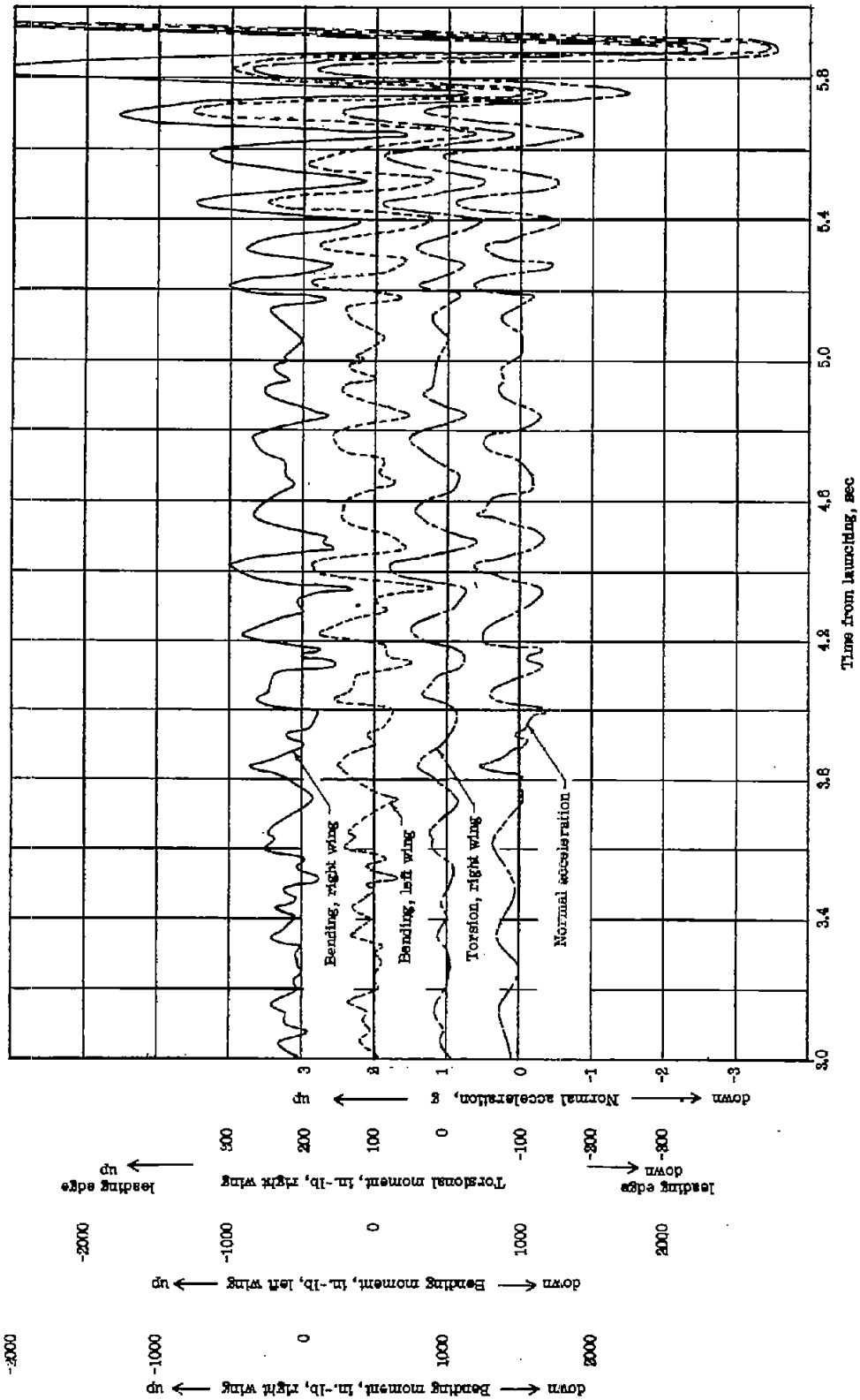

Figure 7.- Portion of telemeter record of model E.

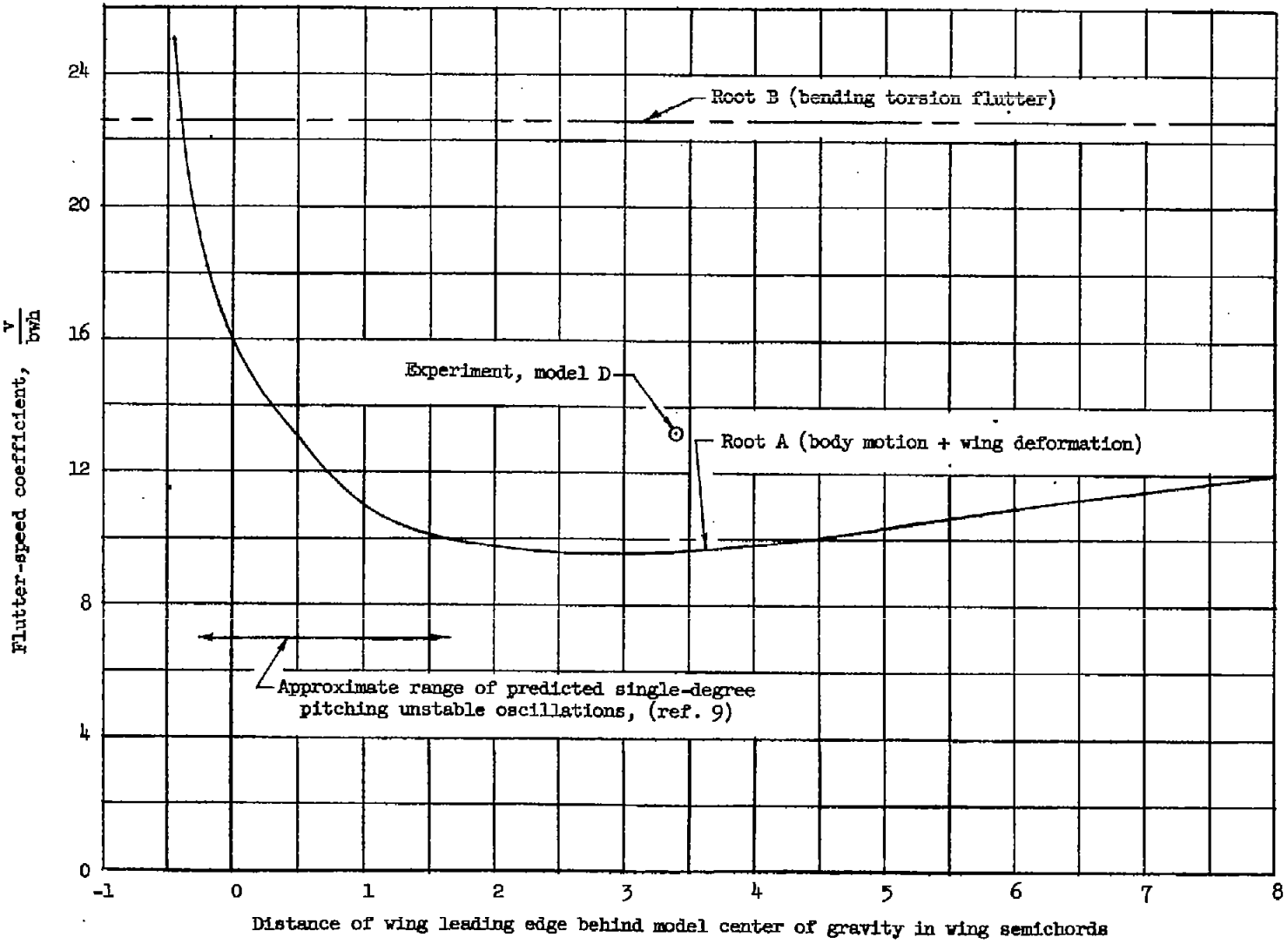

Figure 8.- Variation of flutter-speed coefficient with wing position.

NACA-Langley - 1-12-56 - 100